Reaction Chemistry & Engineering

PAPER

View Article Online
View Journal | View Issue

Cite this: *React. Chem. Eng.*, 2017, **2**, 36

Kinetics of guaiacol deoxygenation using methane over the Pt–Bi catalyst

Yang Xiao and Arvind Varma*

Received 10th October 2016,
Accepted 28th November 2016

DOI: 10.1039/c6re00187d

rsc.li/reaction-engineering

Using H_2 as a reductant, catalytic hydrodeoxygenation (HDO) is typically used for upgrading bio-oils, generally produced from thermal degradation of lignin. In our recent prior work, methane was used to deoxygenate guaiacol over the Pt–Bi catalyst and was found to exhibit as good deoxygenation performance as hydrogen. In the present work, using methane as a reductant, detailed reaction pathways and kinetics of guaiacol deoxygenation are studied using differential and integral operating conditions. Kinetic parameters including rate constants and activation energies are determined for each individual reaction step. The model predicted values match experimental data well. Results from the present work are discussed and compared with the literature values. The present work provides a practical novel approach for bio-oil upgrading using methane as a reductant instead of hydrogen.

Introduction

Energy security and environmental concerns are drivers for utilization of biomass to produce bio-fuels. The vast quantity of biomass available in the United States has the potential to replace significant amounts of fuels that are currently derived from petroleum sources. Bio-oil, generally derived from fast pyrolysis of biomass, is one such candidate fuel.[1] Its production process, however, remains under investigation, owing primarily to its high oxygen content, which may cause instability, poor combustion performance and low heating value.[2–4] Too high levels of oxygen make pyrolysis oils distinctly different from petroleum fuels. Oxygen removal from pyrolyzed bio-oils, thus, is typically followed as an upgrading process to utilize these bio-oils as transportation fuels.[5,6]

Since the pyrolysis bio-oil is always a mixture of more than 400 chemical species and different biomass sources result in different bio-oil compositions, model compounds such as phenol, guaiacol (2-methoxyphenol) and benzylphenyl ether[7] are typically selected to represent bio-oils for more fundamental studies.[8] Among these model compounds, guaiacol is attractive because it contains two common oxygenated groups in bio-oils: hydroxyl and methoxyl. Catalytic hydrodeoxygenation (HDO), as a common bio-oil upgrading approach, refers to oxygen removal by the use of H_2 molecules over heterogeneous catalysts. Using Pt, Pd, Co, *etc.* as primary metals,[9] Mo, S, *etc.* as promoters,[10] and activated carbon (AC), Al_2O_3, ZrO_2, SiO_2, *etc.* as catalyst supports,[11–13] various experimental and theoretical studies have been reported for guaiacol catalytic HDO.[14–20]

Although H_2 is an ideal reductant for oxygen removal from pyrolysis oils, its use in HDO, however, leads to possible economic concerns owing to the high cost of H_2 production and transportation. In some cases, instead of H_2, methane has been used as a reductant. For example, for NO_x to N_2 conversion in the presence of O_2,[21,22] CH_4 was considered as the hydrogen donor and was activated by surface oxygen species.[23]

For these reasons, we have recently reported a novel bio-oil upgrading approach,[24] using CH_4 instead of H_2 as a reductant and Pt–Bi/AC as a catalyst, to deoxygenate guaiacol efficiently. It was found that using the mono-metallic Pt/AC catalyst, CH_4 exhibited good deoxygenation performance as H_2 in terms of guaiacol conversion and product distribution, but the catalyst deactivated rapidly. With addition of bismuth as a promoter, the lifetime of the bi-metallic Pt–Bi/AC was extended significantly without loss of activity, as compared to the Pt/AC catalyst.

In our other prior works,[25,26] using Pt/AC and H_2, reaction pathways and detailed kinetics of the guaiacol deoxygenation process were reported. On the basis of these prior studies,[24–26] in the present work, using methane as the reductant both experimental and modeling investigations were conducted, to reveal the reaction pathways and kinetics of guaiacol deoxygenation, where partially deoxygenated compounds, including phenol and cyclopentanone, are target products. Kinetic measurements in both differential and integral reactors were carried out, and rate constants and activation energy values were determined for the individual reaction steps. These results are discussed and compared with our prior studies as well as other related works.

Davidson School of Chemical Engineering, Purdue University, West Lafayette, IN 47907, USA. E-mail: avarma@purdue.edu; Fax: +1 765 494 0805; Tel: +1 765 494 8484

Experimental

Materials

The 5% Pt–1% Bi/C catalysts were prepared following the procedure described in our prior works.[24,27,28] The metallic precursors were chloroplatinic acid hydrate (99.9% metal basis) and bismuth chloride (99.999%), both from Sigma Aldrich. The 20–120 mesh AC supports were from Norit Americas Inc. Briefly, Pt and Bi were loaded sequentially using the wet impregnation method. First, the Pt and Bi precursors were dissolved in 1.2 mol L^{-1} HCl and then added dropwise to the well-stirred AC slurry, with stirring continued for at least 8 h at room temperature. The mixture was then rinsed and dried in air at 100 °C before use. Guaiacol (>98.0%) and all other calibration compounds (catechol, phenol and cyclopentanone) were purchased from Sigma-Aldrich. GUA, CAT, PHE and CYC are used as abbreviations for guaiacol, catechol, phenol and cyclopentanone, respectively, in the later sections. Ultra high purity grade gases (99.98% oxygen, 99.999% argon, 99.98% helium and 99.999% hydrogen) were purchased from Indiana Oxygen.

The 0.5% Pt/Al_2O_3 (metal dispersion = 31 ± 0.5%) standard (for chemisorption calibration) was from Micromeritics.

Kinetic measurements

The kinetic measurements were conducted in a fixed-bed reactor (316 L stainless steel, inner diameter = 12 mm) setup, described in our prior work.[25,26] Prior to the reaction, the packed catalyst was activated at 400 °C and 1 atm for 4 hours under a gas mixture flow ($H_2:N_2 = 1:2$). The reactor was then purged using N_2 for 30 min. The standard reactor operating conditions were 400 °C, 1 atm, 0.02–0.05 g of catalyst for differential reactions (conversions typically <6–8%) and 0.3–0.5 g of catalyst for integral reactions (conversions typically >20%), total gas ($CH_4:N_2 = 1:1$) flow rate of 100 mL min^{-1}, and guaiacol feed rate of 0.025 mL min^{-1} (liquid, at room temperature).

The feed flow rates correspond to a molar ratio of 10 between CH_4 and guaiacol. Blank tests with co-feeding guaiacol and CH_4/N_2 (1:1) over an AC support with no metal loading were conducted under the standard reaction conditions, and guaiacol conversion was less than 1%, while methane conversion was less than 3%, generating H_2 and trace C_2H_6. This indicates that deoxygenation of guaiacol and methane decomposition to hydrogen/carbon are limited over the inert AC support. All experiments have carbon mass balances of 92 ± 2%, similar to those reported in the literature.[29,30] Possible factors affecting mass balance include liquid hold-up in various locations in the system, particularly the condenser, and coke deposit on the catalyst.

Product analysis

As in our prior works, a GC (Agilent GC6890) with a flame ionization detector (FID), equipped with a DB-1701 column (30 m × 0.25 mm), was used for quantitative analysis of the liquid products.[24–26] The gaseous effluent was analyzed using a Micro GC (Agilent 3000A Micro GC) equipped with two columns (column A, MolSieve 5 A, 10 m × 0.32 mm; column B: Plot U, 8 m × 0.32 mm) and two thermal conductivity detectors (TCD). For the reaction experiments, good repeatability generally within less than 2% deviation was achieved for all quantitative analyses.

Catalyst characterization

Since the same catalyst, as in our prior related work,[24] was used in the present work, catalyst characterization results, including BET surface area, pore diameter, chemisorption (Pt metal dispersion) and transmission electron microscopy, can be found in that article and its Supplementary Information. Briefly, the BET surface areas of Pt–Bi/C are high (>500 m^2 g^{-1}), which imply good capacity to adsorb reactants. The moderate mean pore diameter (about 3 nm) makes the catalyst accessible to larger molecules such as guaiacol (reactant) and catechol. The mean diameters of metal clusters given by TEM (3.3 nm) and chemisorption (3.9 nm) techniques are consistent, providing Pt metal dispersion of Pt–Bi/C by chemisorption of 29%.

Results and discussion

Proposed reaction pathways

Since bismuth and the AC support do not show any activity for guaiacol deoxygenation, platinum is considered as the primary component that catalyzes guaiacol deoxygenation, while surface Pt atoms are the active sites. In our prior work, when

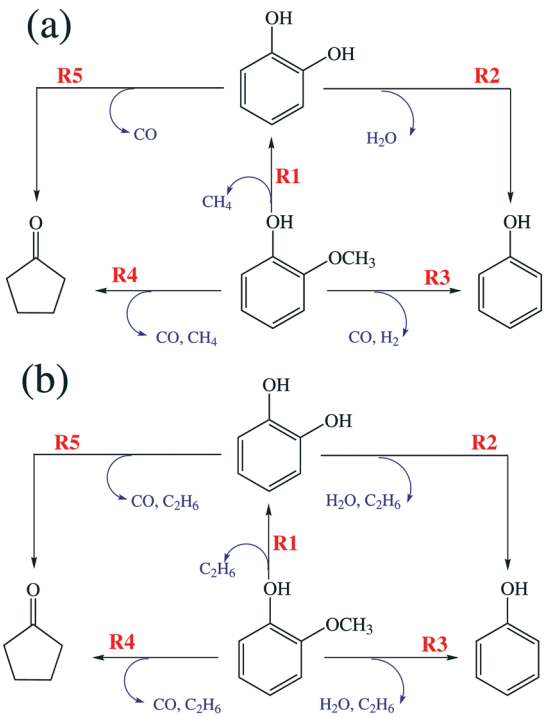

Fig. 1 Proposed reaction pathways of guaiacol deoxygenation for the a) Pt/AC and H_2 case and b) Pt–Bi/AC and CH_4 case.

Pt/AC as a catalyst and H_2 as a reductant were used for guaiacol deoxygenation, reaction pathways, as shown in Fig. 1a, were proposed and confirmed by experimental observations,[25] kinetic modeling and DFT calculations.[26] Similar reaction pathways, as shown in Fig. 1b, apply in the present work since the same product species, including GUA, CAT, PHE and CYC, and similar distribution are found when Pt–Bi/AC as a catalyst and CH_4 as a reductant are used. Both Fig. 1a and b describe reaction pathways containing five individual steps, denoted as R1–R5, producing catechol, phenol and cyclopentanone as liquid products, while different gaseous by-products arise from H_2 and CH_4, respectively. It is proposed that the same active site (surface Pt) is effective for all the five steps (R1–R5). Experimentally, no significant conversion was found when phenol and cyclopentanone were used as reactants in the feed, indicating no additional reactions beyond steps R1–R5.

Based on the above features, detailed reactions between guaiacol/intermediates and methane are proposed in Fig. 2.

For a deoxygenation reaction (such as R2 or R3), similar to H_2, one molecule of CH_4 provides only one H atom to oxygen-containing groups, forming H_2O or other hydrogenated species, while the residual CH_3 combines with another CH_3 to form a C_2H_6 molecule.

Absence of mass transfer limitations

Before conducting kinetic measurements, mass transfer limitations were tested in a differential reactor, using the well-known procedure.[31] The experimental results are shown in Fig. 3.

Fig. 3a is obtained by varying the packed catalyst particle diameter (d_p) in the range 100 microns $< d_p <$ 1000 microns, while keeping other operating conditions (guaiacol flow rate = 1.8 mL h^{-1}) unchanged. Fig. 3b is obtained by varying the guaiacol feed flow rates, while maintaining contact time (W/F) and other operating conditions constant ($d_p <$ 150 microns). Fig. 3a shows that when the catalyst particle diameter (d_p) is larger than 250 microns, corresponding to 60 mesh, internal diffusion effects are discerned, while when (d_p) $<$ 150 microns, corresponding to 100 mesh, no significant internal effects are found. As shown in Fig. 3b, when the feed flow rate is smaller than 1.2 mL min^{-1}, there is an obvious external mass transfer effect, while no such effect is observed when the feed flow rate is larger than 1.5 mL min^{-1}. Thus, d_p = 100 microns and a feed flow rate larger than 1.5 mL min^{-1} were used in the kinetic measurement experiments. Further, the criteria described by Weisz and Prater[32] and Mears[33] were both satisfied to verify the absence of mass and heat transfer effects in all experiments.

Kinetic model development

The reaction rates of step Ri in Fig. 1b and the corresponding turnover frequencies (TOF) are defined by eqn (1) and (2), respectively

$$r_i = \frac{\mathrm{d}F}{\mathrm{d}W} \tag{1}$$

$$\mathrm{TOF}_i = \frac{\mathrm{d}F}{\mathrm{d}(\text{active site})} = r_i \times \frac{M_{\mathrm{Pt}}}{\mathrm{wt\%} \cdot \mathrm{D\%}} \tag{2}$$

Since only one catalyst (Pt–Bi/AC), with a specific Pt metal loading amount (wt% = 5%) and a specific Pt metal dispersion (D% = 29%), was used in the kinetic experiments, the reaction rate and TOF are inter-converted as indicated in eqn (1) and (2).

The reaction pathways, including five individual steps (R1–R5) as shown in Fig. 1b, were established under integral operating conditions. When using guaiacol as the feed, under differential operating conditions (guaiacol conversion less than 6–8%), catechol is the only detectable product, *i.e.* only step R1 prevails while steps R3 and R4 are negligible. This is likely due to lower reaction rates, hence lower yields (smaller than 6–8%) of steps R3 and R4, as compared to step R1.

When catechol is used as feed, also under differential conditions, both phenol and cyclopentanone (corresponding to steps R2 and R5) exist in the liquid products. These experimental observations imply that when guaiacol is fed under differential operating conditions, R1 is faster than R3 and

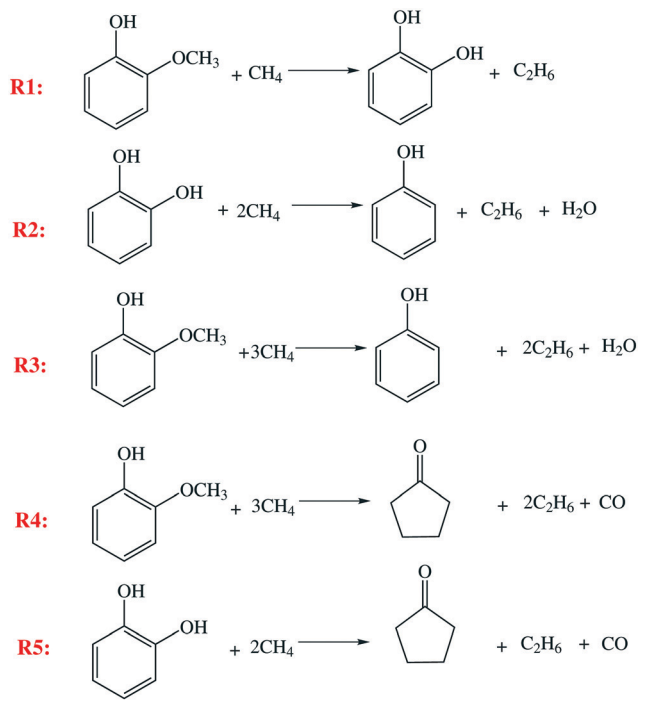

Fig. 2 Detailed reactions between guaiacol/intermediates and methane.

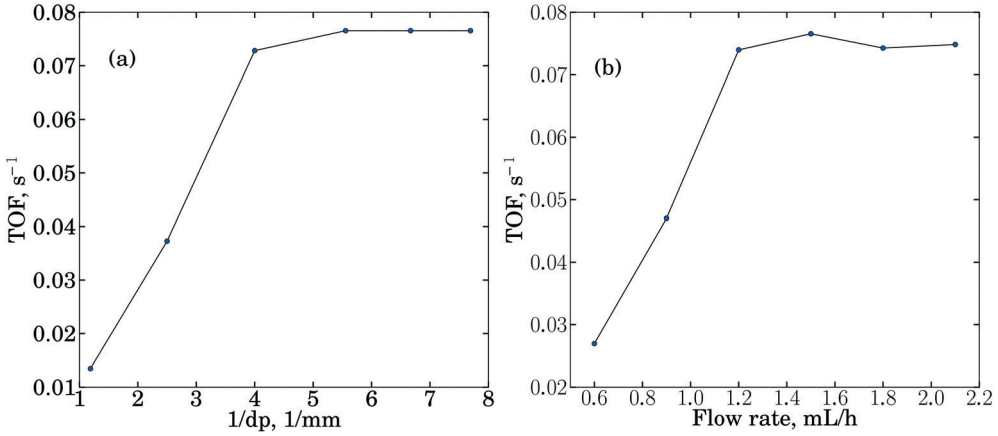

Fig. 3 Mass transfer limitation tests for the a) internal diffusion effect and b) external diffusion effect.

R4, and phenol and cyclopentanone are not produced owing to the low concentration of catechol. Therefore, kinetic parameters for steps R1, R2 and R5 could be obtained by running differential reactions. Using kinetic parameters of R1, R2 and R5, those for R3 and R4 could be further regressed by running integral reactions.

When differential operating conditions apply, reaction rates are obtained using eqn (3).

$$r_i = F_0 \times \frac{X}{W} \tag{3}$$

Based on the design equation for a fixed-bed reactor and the proposed pathways in Fig. 1b, consumption/formation rates of guaiacol, catechol, phenol and cyclopentanone are shown in eqn (4)–(7).

$$\frac{dF_{GUA}}{dW} = -r_1 - r_3 - r_4 \tag{4}$$

$$\frac{dF_{CAT}}{dW} = r_1 - r_2 - r_5 \tag{5}$$

$$\frac{dF_{CYC}}{dW} = r_4 + r_5 \tag{6}$$

$$\frac{dF_{PHE}}{dW} = r_2 + r_3 \tag{7}$$

An overall material balance yields the following equations (eqn (8) and (9)):

$$F_{GUA} + F_{CAT} + F_{CYC} + F_{PHE} = F_0 \tag{8}$$

$$P_i = F_i \times \frac{P_0}{F_0} \tag{9}$$

As described in the kinetic measurements section, excess methane (the molar ratio of methane to reactants is ~10 : 1) is used in all cases, thus partial pressure of methane may be considered as a constant contribution to the reaction rate expressions. The following data fitting and optimization are based on experimental measurements at various temperatures from 325 to 450 °C. Although only results at 400 °C are shown below because this standard operating temperature gives the optimum deoxygenation performance of guaiacol[24] and results at 400 °C were repeated more than 5 times, fitting and optimization results for different temperatures give similar conclusions. All experiments at other temperatures were repeated at least twice and are discussed in the section on Activation energies and temperature effect.

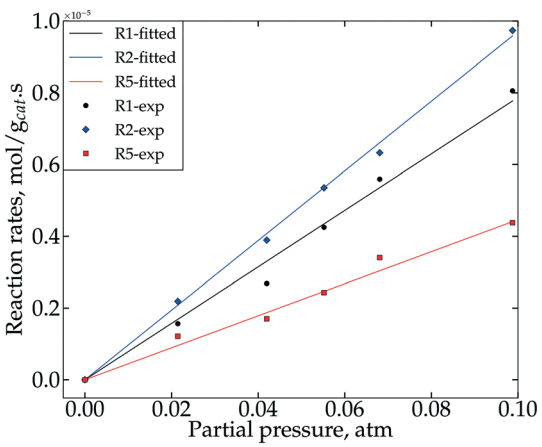

Fig. 4 Reaction rate fits for steps R1, R2 and R5 at 400 °C.

Table 1 Reaction rate constants for steps R1, R2 and R5 at 400 °C; units of k_i, mol g_{cat}^{-1} s^{-1} atm^{-1}

Steps	$k_i \times 10^{-5}$
R1	8.29 ± 0.07
R2	9.71 ± 0.03
R5	4.47 ± 0.03

Differential reactions for steps R1, R2 and R5

When differential operating conditions apply at 400 °C, for steps R1, R2 and R5, the corresponding reaction rates r_1, r_2 and r_5 were obtained using eqn (3).

Using different feed partial pressures of guaiacol or catechol, reaction rates were measured and plotted with respect to average bed reactant partial pressures (average pressures of the inlet and outlet), as shown in Fig. 4. All three data sets follow linear regressions, indicating first order kinetics for steps R1, R2 and R5. Thus, the corresponding reaction rates at 400 °C are described using eqn (10)–(12), where the regressed values of k_1, k_2 and k_5 are listed in Table 1. The reaction rate regressions of R1, R2 and R5 at other temperatures are also essentially linear, as discussed later in the section on Activation energies and temperature effect.

$$r_1 = k_1 P_{GUA} \quad (10)$$

$$r_2 = k_2 P_{CAT} \quad (11)$$

$$r_5 = k_5 P_{CAT} \quad (12)$$

Using H_2 as a reductant, Runnebaum *et al.*[34] also reported 1st order kinetics for step R1 over the Pt/Al_2O_3 catalyst, while our prior work[26] fitted a 2nd order for the same step. The difference between the present work and our prior work may be due to different reductants (H_2 or CH_4). For steps R2 and R5, both the present work and our prior work demonstrate 1st order kinetics. The reaction rate constant values, however, are smaller when CH_4 is used as a reductant, indicating a higher activation energy for CH_4.

Integral reactions of steps R3 and R4

As shown above, under differential operating conditions, step R1 is decomposed from the reaction network (Fig. 1) when guaiacol is fed over the catalyst. Similarly, steps R2 and R5 are decomposed under differential operating conditions when catechol is fed. To obtain insight into steps R3 and R4, integral operating conditions (guaiacol conversion >30%) were used while guaiacol is fed by packing more catalyst, producing distinct amounts of phenol and cyclopentanone. These, obviously, introduce not only steps R3 and R4 but also steps R1, R2 and R5. It should be clear that the integral operating conditions do not create new pathways (steps R3 and R4), as compared to the differential operating conditions (only step R1). Instead, under differential operating conditions, owing to low guaiacol conversion (6–8%), undetectability of products (PHE and CYC, estimated amount <2%) from steps R3 and R4 is due to the GC equipment detection limit and unavoidable loss during product collection and analysis. These limitations were overcome by higher guaiacol conversion under integral operating conditions.

Since all five steps (R1 to R5) exist under integral operating conditions, eqn (4)–(7) can be re-written as eqn (13)–(16), where k_i and n_i are reaction rate constants and orders for steps R*i*.

$$\frac{dF_{GUA}}{dW} = -r_1 - r_3 - r_4 = -k_1 P_{GUA}^{n_1} - k_3 P_{GUA}^{n_3} - k_4 P_{GUA}^{n_4} \quad (13)$$

$$\frac{dF_{CAT}}{dW} = r_1 - r_2 - r_5 = -k_1 P_{GUA}^{n_1} - k_2 P_{CAT}^{n_2} - k_5 P_{CAT}^{n_5} \quad (14)$$

$$\frac{dF_{CYC}}{dW} = r_4 + r_5 = k_4 P_{GUA}^{n_4} + k_5 P_{CAT}^{n_5} \quad (15)$$

$$\frac{dF_{PHE}}{dW} = r_2 + r_3 = k_2 P_{CAT}^{n_2} + k_3 P_{GUA}^{n_3} \quad (16)$$

In this description, the reaction orders for steps 1, 2 and 5 are also kept flexible. With k_i and n_i as variables (total 10), predicted values of flow rates for GUA, CAT, CYC and PHE can be calculated by Runge–Kutta numerical integration using the following initial conditions:

$$F_{GUA} = F_0,\ F_{CAT} = 0,\ F_{PHE} = 0 \text{ and } F_{CYC} = 0, \text{ when } W = 0. \quad (17)$$

In general, for parameter estimation involving exponents, the weighted least-squares method is recommended and was followed in the present work.[35–37] This involves minimizing the error estimate given by eqn (18).

$$\sigma^2 = \sum_i w_i (F_{exp_i} - F_{pred_i})^2, \quad (18)$$

where i = GUA, CAT, PHE and CYC if integral conditions apply, while i = GUA and CAT if differential conditions apply,

Table 2 Optimized n_i and k_i values for $w_i = F_i^2$; units of k_i, mol $g_{cat}^{-1} s^{-1} atm^{-n_i}$

n_1	n_2	n_3	n_4	n_5	$k_1 \times 10^{-5}$	$k_2 \times 10^{-5}$	$k_3 \times 10^{-5}$	$k_4 \times 10^{-5}$	$k_5 \times 10^{-5}$
1.00	1.00	2.00	2.00	1.00	8.38	9.68	23.8	1.76	4.46

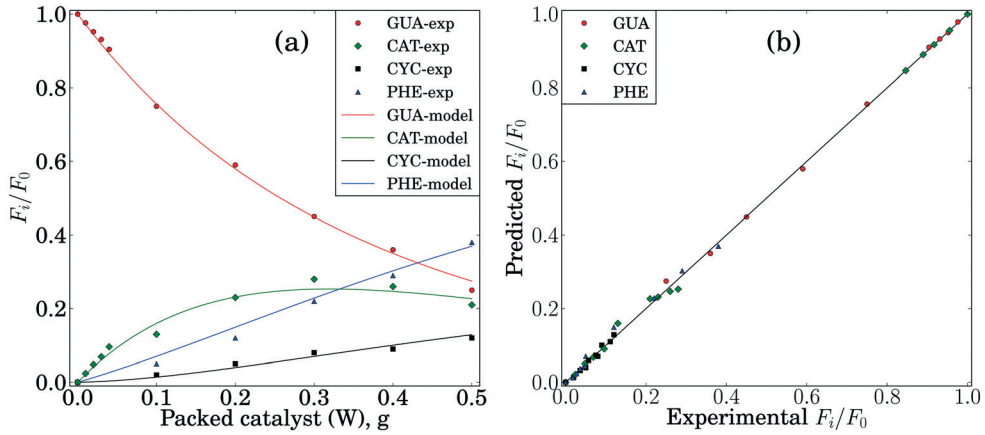

Fig. 5 A comparison of experimental and predicted flow rate values for a) different catalyst amounts and b) parity plot.

and w_i are the weighting functions. In principle, any positive weighting function can be used. For single reactions, the appropriate w_i have been reported by de Levie[38] but are not available for a simultaneous multi-reaction network, as in the present case. Following de Levie, $w_i = 1$, F_i^2, F_i^4 and F_i^6 are appropriate for single reactions with orders of 0, 1, 2 and 3, respectively.[38]

Since the differential reaction analysis yielded first-order kinetics for steps R1, R2 and R5, we used $w_i = F_i^2$ as the starting weighting functions. A sequential optimization strategy was then employed where only 2 (k_3 and k_4) or 4 (k_3, k_4, n_3 and n_4) variables out of 10 were kept flexible at the initial stage. Using these results as initial guesses, all 10 variables were allowed to vary in the final stage and the corresponding optimized parameters are shown in Table 2. Since the reaction orders n_3 and n_4 are 2, $w_i = F_i^4$ was also tested and converged to the same n_i as for $w_i = F_i^2$ and essentially the same k_i values as well. Thus, it appears that $w_i = F_i^2$ is an appropriate choice for the weighting function.

Using data from both integral and differential operating conditions, a comparison of the experimental and predicted flow rates is shown in Fig. 5. Fig. 5a shows that predicted flow rates are close to the experimental values for various catalyst amounts. Fig. 5b summarizes the goodness-of-fit in a parity plot. The values for all species are close to the diagonal line and relatively evenly distributed on both sides, indicating a good fit (normalized RMS error = 2.8%).

Because both experimental observations and kinetic modeling indicate that r_1 is larger than both r_3 and r_4, it is worthwhile to test a reduced model with R3 and R4 steps excluded, which means that $k_3 = 0$ and $k_4 = 0$. The results, however, show that the reduced model (RMS error = 11.4%) does not fit the experimental data as well as the full model. Thus, steps R3 and R4 are important and cannot be neglected to predict the product distribution for guaiacol deoxygenation over the Pt–Bi/AC catalyst.

Activation energies and temperature effect

In the above sections, all reaction orders and rate constants at 400 °C were determined. Using the Arrhenius equation (eqn (19)), reaction activation energies (E_a) and exponential factors (A) were calculated.

$$k = A\exp\left(-\frac{E_a}{RT}\right) \tag{19}$$

The E_a values are listed in Table 3 and also compared with our prior work,[26] where hydrogen and Pt/AC were used.

The activation energy of step R1 was reported to be 71.2, 58.7 and 89.1 kJ mol^{-1} for Co–Mo, Ni–Mo and Ni–Cu catalysts, respectively,[39,40] when H_2 was used as a reductant. There are no data available for the CH_4 case in the literature. Using Pt-based catalysts, our activation energies of step R1 are 146 and 126 kJ mol^{-1} for the CH_4 and H_2 cases, respectively, both higher than the literature data. The difference is likely due to the catalyst itself, including Pt metal nature, Pt particle size, support effect and Bi promoter addition.[24,41] Table 3 also shows that activation energies for the CH_4 case are always 10–35 kJ mol^{-1} higher (except R3) than those for the H_2 case. This is an explanation for the fact that, to achieve a similar guaiacol conversion at 300 °C for the H_2 case, 400 °C is needed for the CH_4 case as shown in our prior work.[24] For step R3, activation energy of the H_2 case is only 93 kJ mol^{-1}, while it is 166 kJ mol^{-1} for the CH_4 case. This is likely because H_2 promotes step R3 by forming a more stable by-product, *i.e.* CO than C_2H_6, the by-product from the CH_4 case.

With the kinetics fully known, it is now possible to see how well they fit the entire data set for all temperature, flow rate and pressure conditions investigated in this work (total of 140 data points for species concentrations). The entire

Table 3 Reaction activation energy values, along with the comparison for CH_4 and H_2 cases

E_a, kJ mol^{-1}	R_1	R_2	R_3	R_4	R_5
CH_4 case	146 ± 11	110 ± 8	166 ± 13	184 ± 14	141 ± 9
H_2 case	126 ± 6	100 ± 4	93 ± 3	149 ± 5	125 ± 2

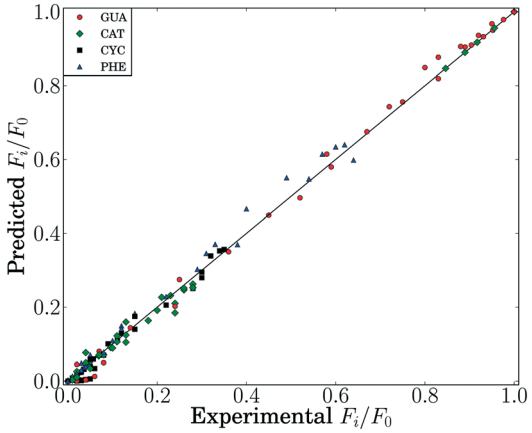

Fig. 6 The parity plot of all investigated data.

data set is shown in the parity plot in Fig. 6, where the RMS error = 5.7%, indicating a good fit.

Concluding remarks

In the present work, kinetics of guaiacol deoxygenation using methane as a reductant over the Pt–Bi/AC catalyst is studied by both experimental and modeling approaches. It is shown that the liquid phase products remain the same as for the case using hydrogen as a reductant.[26] The activation energies and other kinetic parameters are obtained based on data fit. For all the temperature, flow rate and pressure conditions investigated in this work, the model predictions match the experimental data well. Modeling results are discussed, analyzed and compared with literature reports. The present work provides a new practical approach for bio-oil upgrading using methane as a reductant instead of hydrogen.

Nomenclature

A_i [mol s^{-1} g_{cat}^{-1}]	Pre-exponential factor of step i
D%	Metal dispersion
E_{a_i} [kJ mol^{-1}]	Activation energy of step i
F_0 [mol h^{-1}]	Feed flow rate
F_i [mol h^{-1}]	Flow rate of species i
k_i [mol g_{cat}^{-1} s^{-1} atm^{-n}]	Reaction rate constant of step i when the reaction order is n
M_{Pt} [kg $kmol^{-1}$]	Molecular weight of Pt
N_i [mol]	Amount of species i
n_i [mol]	Reaction order of step i
P_i [atm]	Partial pressure of species i
R [J K^{-1} mol^{-1}]	Gas constant
r_i [mol s^{-1} g_{cat}^{-1}]	Reaction rate of step i
t [s]	Contact time
TOF_i [s^{-1}]	Turnover frequency of step i
W [g]	Catalyst packing amount
w_i [—]	Weighting function for species i
wt%	Metal loading percentage

Acknowledgements

This work was supported by the R. Games Slayter Fund. The authors thank Ms. Marina Lourencone for her valuable assistance.

References

1 C. O. Tuck, E. Pérez, I. T. Horváth, R. A. Sheldon and M. Poliakoff, Valorization of Biomass: Deriving More Value from Waste, *Science*, 2012, **337**, 695–699.
2 P. S. Nigam and A. Singh, Production of liquid biofuels from renewable resources, *Prog. Energy Combust. Sci.*, 2011, **37**, 52–68.
3 D. C. Elliott and T. R. Hart, Catalytic Hydroprocessing of Chemical Models for Bio-oil, *Energy Fuels*, 2009, **23**, 631–637.
4 P. Mortensen, J.-D. Grunwaldt, P. Jensen, K. Knudsen and A. Jensen, A Review of Catalytic Upgrading of Bio-oil to Engine Fuels, *Appl. Catal., A*, 2011, **407**, 1–19.
5 S. Xiu and A. Shahbazi, Bio-oil Production and Upgrading Research: A Review, *Renewable Sustainable Energy Rev.*, 2012, **16**, 4406–4414.
6 D. C. Elliott, H. Wang, M. Rover, L. Whitmer, R. Smith and R. Brown, Hydrocarbon Liquid Production via Catalytic Hydroprocessing of Phenolic Oils Fractionated from Fast Pyrolysis of Red Oak and Corn Stover, *ACS Sustainable Chem. Eng.*, 2015, **3**, 892–902.
7 B. Guvenatam, O. Kursun, E. H. Heeres, E. A. Pidko and E. J. Hensen, Hydrodeoxygenation of Mono- and Dimeric lignin Model Compounds on Noble Metal Catalysts, *Catal. Today*, 2014, **233**, 83–91.
8 A. Bridgwater, Review of Fast Pyrolysis of Biomass and Product Upgrading, *Biomass Bioenergy*, 2012, **38**, 68–94.
9 J. Wildschut, F. H. Mahfud, R. H. Venderbosch and H. J. Heeres, Hydrotreatment of Fast Pyrolysis Oil Using Heterogeneous Noble-metal Catalysts, *Ind. Eng. Chem. Res.*, 2009, **48**, 10324–10334.
10 W. Wang, Y. Yang, H. Luo, H. Peng and F. Wang, Effect of La on Ni–W–B Amorphous Catalysts in Hydrodeoxygenation of Phenol, *Ind. Eng. Chem. Res.*, 2011, **50**, 10936–10942.
11 A. Gutierrez, R. Kaila, M. Honkela, R. Slioor and A. Krause, Hydrodeoxygenation of Guaiacol on Noble Metal Catalysts, *Catal. Today*, 2009, **147**, 239–246.
12 M. Saidi, F. Samimi, D. Karimipourfard, T. Nimmanwudipong, B. C. Gates and M. R. Rahimpour, Upgrading of Lignin-derived Bio-oils by Catalytic Hydrodeoxygenation, *Energy Environ. Sci.*, 2014, **7**, 103–129.
13 S.-K. Wu, P.-C. Lai, Y.-C. Lin, H.-P. Wan, H.-T. Lee and Y.-H. Chang, Atmospheric Hydrodeoxygenation of Guaiacol over Alumina-, Zirconia-, and Silica-supported Nickel Phosphide Catalysts, *ACS Sustainable Chem. Eng.*, 2013, **1**, 349–358.
14 H. Zhao, D. Li, P. Bui and S. Oyama, Hydrodeoxygenation of Guaiacol as Model Compound for Pyrolysis Oil on Transition Metal Phosphide Hydroprocessing Catalysts, *Appl. Catal., A*, 2011, **391**, 305–310.

15 V. N. Bui, D. Laurenti, P. Afanasiev and C. Geantet, Hydrodeoxygenation of Guaiacol with CoMo Catalysts. Part I: Promoting Effect of Cobalt on HDO Selectivity and Activity, *Appl. Catal., B*, 2011, **101**, 239–245.
16 X. Zhang, T. Wang, L. Ma, Q. Zhang, Y. Yu and Q. Liu, Characterization and Catalytic Properties of Ni and NiCu Catalysts Supported on ZrO_2–SiO_2 for Guaiacol Hydrodeoxygenation, *Catal. Commun.*, 2013, **33**, 15–19.
17 T. Mochizuki, S.-Y. Chen, M. Toba and Y. Yoshimura, Deoxygenation of Guaiacol and Woody Tar over Reduced Catalysts, *Appl. Catal., B*, 2014, **146**, 237–243.
18 R. Olcese, M. Bettahar, D. Petitjean, B. Malaman, F. Giovanella and A. Dufour, Gas-phase Hydrodeoxygenation of Guaiacol Over Fe/SiO_2 Catalyst, *Appl. Catal., B*, 2012, **115-116**, 63–73.
19 M. Badawi, J.-F. Paul, S. Cristol and E. Payen, Guaiacol Derivatives and Inhibiting Species Adsorption over MoS_2 and CoMoS Catalysts under HDO Conditions: A DFT study, *Catal. Commun.*, 2011, **12**, 901–905.
20 K. Lee, G. H. Gu, C. A. Mullen, A. A. Boateng and D. G. Vlachos, Guaiacol Hydrodeoxygenation Mechanism on Pt(111): Insights from Density Functional Theory and Linear Free Energy Relations, *ChemSusChem*, 2015, **8**, 315–322.
21 E. Kikuchi, M. Ogura, I. Terasaki and Y. Goto, Selective Reduction of Nitric Oxide with Methane on Gallium and Indium Containing H-ZSM-5 Catalysts: Formation of Active Sites by Solid-State Ion Exchange, *J. Catal.*, 1996, **161**, 465–470.
22 S. Burns, J. Hargreaves and S. Hunter, On the Enhancing Effect of Ce in Pd-MOR Catalysts for NO_x CH_4-SCR: A Structure-reactivity Study, *Appl. Catal., B*, 2016, **195**, 121–131.
23 H. Pan, Y. Jian, Y. Yu, N. Chen, C. He and C. He, Promotional Mechanism of Propane on Selective Catalytic Reduction of NO_x by Methane over In/H-BEA at Low Temperature, *Appl. Surf. Sci.*, 2016, **390**, 608–616.
24 Y. Xiao and A. Varma, Catalytic Deoxygenation of Guaiacol Using Methane, *ACS Sustainable Chem. Eng.*, 2015, **3**, 2606–2610.
25 D. Gao, C. Schweitzer, H. T. Hwang and A. Varma, Conversion of Guaiacol on Noble Metal Catalysts: Reaction Performance and Deactivation Studies, *Ind. Eng. Chem. Res.*, 2014, **53**, 18658–18667.
26 D. Gao, Y. Xiao and A. Varma, Guaiacol Hydrodeoxygenation over Platinum Catalyst: Reaction Pathways and Kinetics, *Ind. Eng. Chem. Res.*, 2015, **54**, 10638–10644.
27 W. Hu, D. Knight, B. Lowry and A. Varma, Selective Oxidation of Glycerol to Dihydroxyacetone over Pt-Bi/C Catalyst: Optimization of Catalyst and Reaction Conditions, *Ind. Eng. Chem. Res.*, 2010, **49**, 10876–10882.
28 W. Hu, B. Lowry and A. Varma, Kinetic Study of Glycerol Oxidation Network over Pt-Bi/C Catalyst, *Appl. Catal., B*, 2011, **106**, 123–132.
29 J. Chang, T. Danuthai, S. Dewiyanti, C. Wang and A. Borgna, Hydrodeoxygenation of Guaiacol over Carbon-supported Metal Catalysts, *ChemCatChem*, 2013, **5**, 3041–3049.
30 A. L. Jongerius, P. C. A. Bruijnincx and B. M. Weckhuysen, Liquid-phase Reforming and Hydrodeoxygenation as a Two-step Route to Aromatics from Lignin, *Green Chem.*, 2013, **15**, 3049–3056.
31 C. Perego and S. Peratello, Experimental Methods in Catalytic Kinetics, *Catal. Today*, 1999, **52**, 133–145.
32 P. Weisz and C. Prater, Interpretation of Measurements in Experimental Catalysis, *Adv. Catal.*, 1954, **6**, 143–196.
33 D. E. Mears, Diagnostic Criteria for Heat Transport Limitations in Fixed Bed Reactors, *J. Catal.*, 1971, **20**, 127–131.
34 R. C. Runnebaum, T. Nimmanwudipong, D. E. Block and B. C. Gates, Catalytic Conversion of Compounds Representative of Lignin-derived Bio-oils: a Reaction Network for Guaiacol, Anisole, 4-Methylanisole, and Cyclohexanone Conversion Catalysed by Pt/γ-Al_2O_3, *Catal. Sci. Technol.*, 2012, 113–118.
35 A. C. Norris, *Computational Chemistry: An Introduction to Numerical Methods*, Wiley, New York, 1981.
36 H. S. Fogler, *Elements of Chemical Reaction Engineering*, 4th edn, Prentice Hall International, Inc, New Jersey, 2005.
37 G. E. P. Box, J. S. Hunter and W. G. Hunter, *Statistics for Experimenters: Design, Innovation, and Discovery*, 2nd edn, Wiley, New Jersey, 2005.
38 R. de Levie, When, Why, and How to Use Weighted Least Squares, *J. Chem. Educ.*, 1986, **63**, 10.
39 E. Laurent and B. Delmon, Study of the Hydrodeoxygenation of Carbonyl, Carboxylic and Guaiacyl Groups over Sulfided CoMo/γ-Al_2O_3 and NiMo/γ-Al_2O_3 catalyst, *Appl. Catal., A*, 1994, **109**, 97–115.
40 M. V. Bykova, S. G. Zavarukhin, L. I. Trusov and V. A. Yakovlev, Guaiacol Hydrodeoxygenation Kinetics with Catalyst Deactivation Taken into Consideration, *Kinet. Catal.*, 2013, **54**, 40–48.
41 A. K. Deepa and P. L. Dhepe, Function of Metals and Supports on the Hydrodeoxygenation of Phenolic Compounds, *ChemPlusChem*, 2014, **79**, 1573–1583.